

Supplementary Information

Figure S.1: Graphs showing the relative percentage (% total calcareous) distributions of the abundant living benthic foraminifera.

Figure S.2: *Q*-mode hierarchical cluster analysis (UPGMA Bray-Curtis similarity index) applied on living taxa.

Figure S.3: Canonical Correspondence Analysis (CCA) results applied to living foraminifera census dataset. Blue dots indicate the species and crosses indicate the samples. Abundant species included in the quantification approach together with species mentioned in the text are shown in bold and with their names.

Table S.1: Results of bottom-water oxygenation estimations ($[O_2]_{BW}$) in 3 sediment cores with the core depth and calibrated age point information.

Figure S.1. Graph showing the relative percentage (% total calcareous) distributions of abundant living benthic foraminifera. X-axis indicates the stations (water depth(m)) which are grouped according to the prevailing bottom.-water-oxygen concentrations (black for microoxic (<5 $\mu\text{mol/kg}$), orange for dysoxic (5-45 $\mu\text{mol/kg}$), green for oxic (>45 $\mu\text{mol/kg}$)).

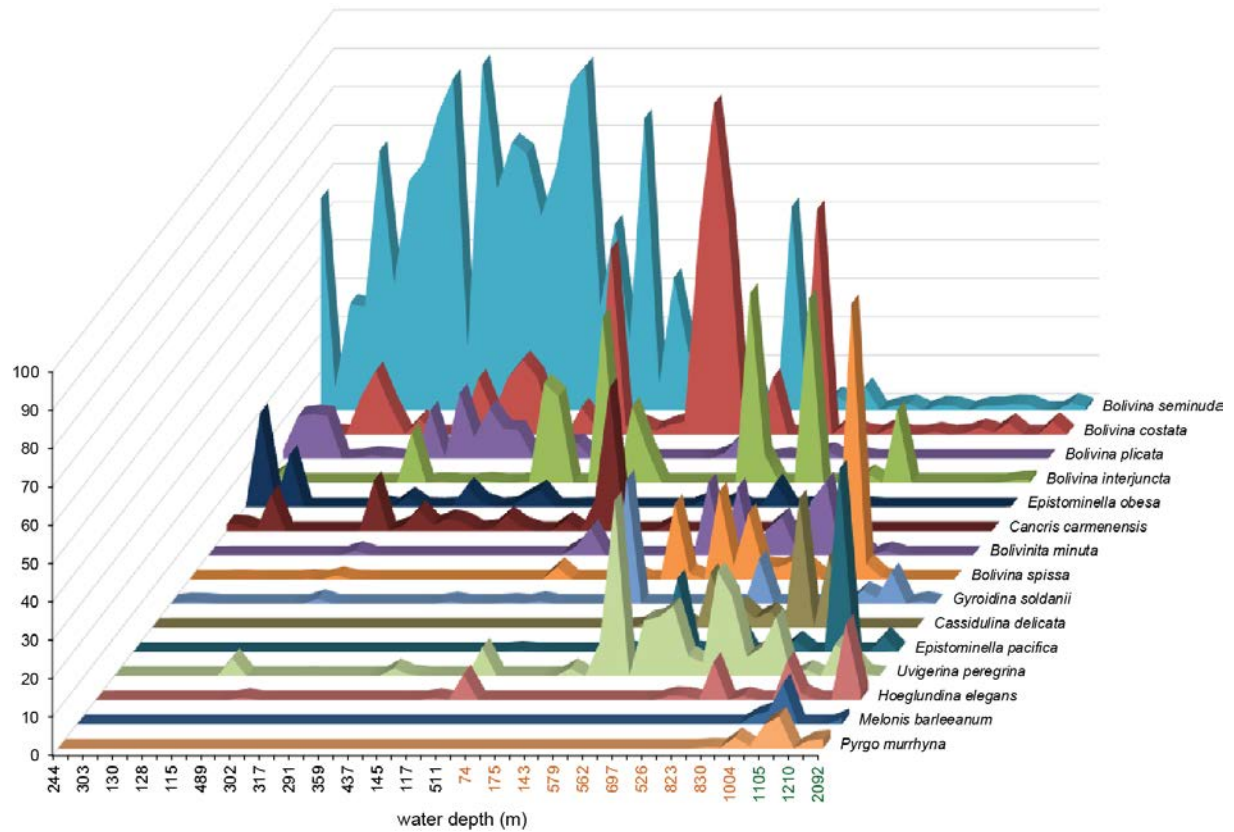


Figure S.2: Q-mode hierarchical cluster analysis (UPGMA Bray-Curtis similarity index) applied on living taxa.

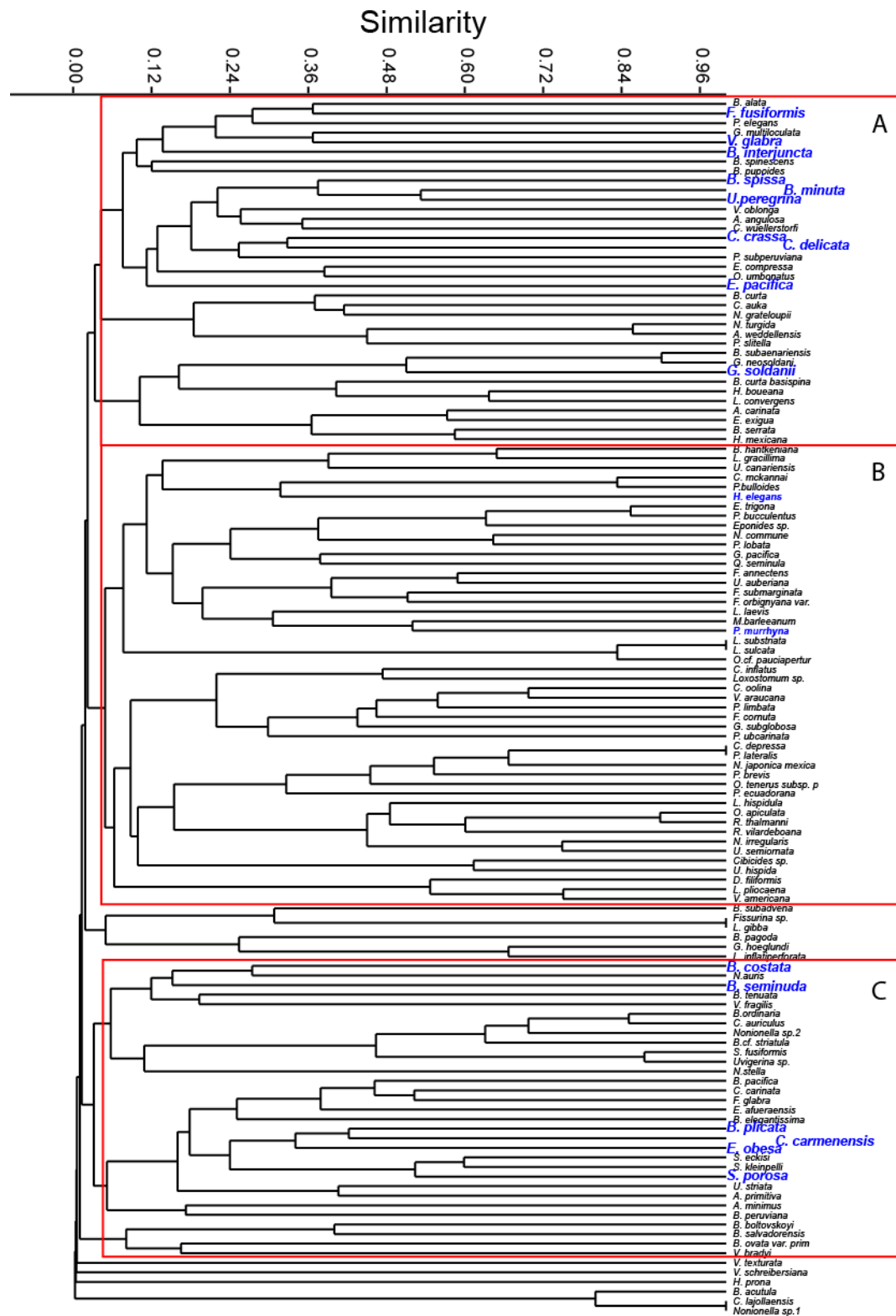
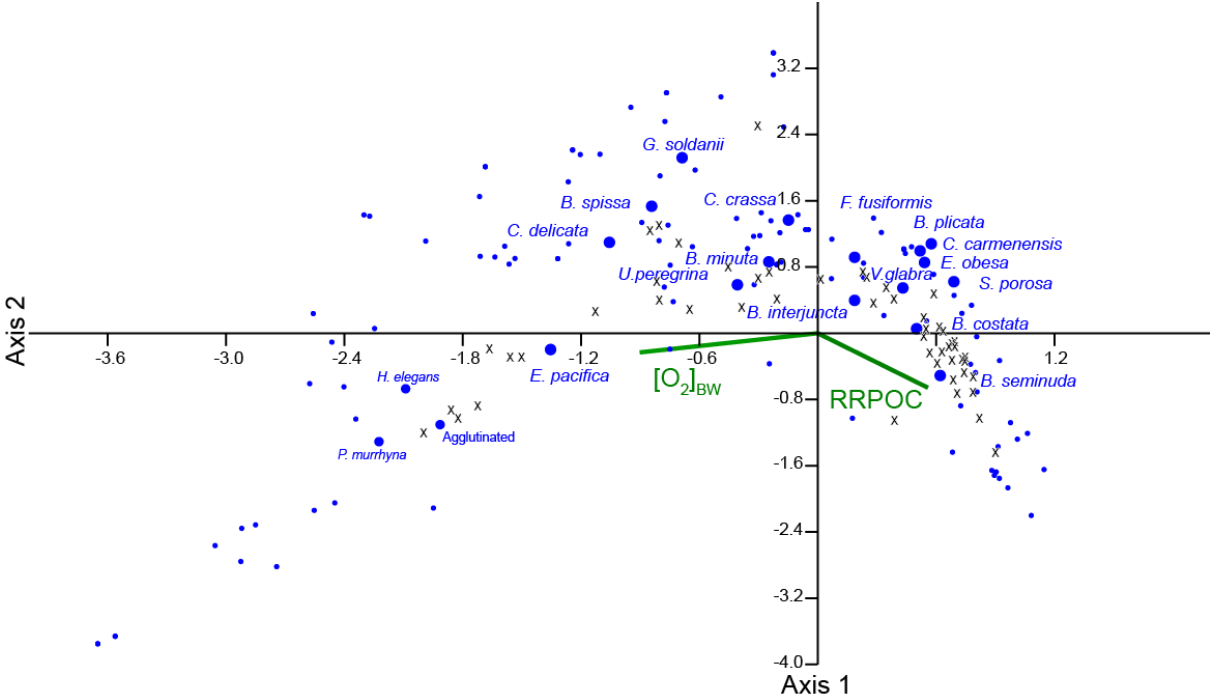


Figure S.3: Canonical Correspondence Analysis (CCA) results applied to living foraminifera census dataset. Blue dots indicate the species and crosses indicate the samples. Abundant species included in the quantification approach together with species mentioned in the text are shown in bold and with their names.



Supplementary information Table 1. Results of bottom-water oxygenation estimations ($[O_2]_{BW}$) in 3 sediment cores with the core depth and calibrated age point information.

| | M77/2-50-4 8°S 1013 m | | | | M77/2-52-2 5°S 1249 m | | | | M77/2-59-1 3°57'S 997 m | | | |
|--------------------|-----------------------|------------------|-------------------------------------|-------|-----------------------|------------------|-------------------------------------|-------|-------------------------|------------------|-------------------------------------|-------|
| | Core depth (cm) | Age (cal yrs BP) | $[O_2]_{BW}$ ($\mu\text{mol/kg}$) | error | Core depth (cm) | Age (cal yrs BP) | $[O_2]_{BW}$ ($\mu\text{mol/kg}$) | error | Core depth (cm) | Age (cal yrs BP) | $[O_2]_{BW}$ ($\mu\text{mol/kg}$) | error |
| late Holocene | HIATUS | | | | 90 | 3130 | 32.40 | 12.42 | 143 | 3024 | 8.91 | 21.88 |
| | | | | | 110 | 3845 | 25.58 | 14.18 | 163 | 3413 | 6.79 | 22.14 |
| | | | | | 120 | 4202 | 31.01 | 12.11 | 183 | 3801 | -9.91 | 28.54 |
| | | | | | 130 | 4559 | 23.29 | 14.41 | 203 | 4178 | 3.84 | 22.85 |
| | | | | | 140 | 4917 | 31.30 | 11.98 | 223 | 4531 | 11.36 | 20.88 |
| | | | | | | | | | 243 | 4877 | 25.37 | 15.68 |
| early Holocene | HIATUS | | | | 230 | 8097 | 13.67 | 16.88 | 403 | 8098 | 30.76 | 14.64 |
| | | | | | 240 | 8486 | 18.43 | 14.22 | 443 | 8596 | 22.20 | 17.46 |
| | | | | | 250 | 8839 | 30.15 | 12.15 | 483 | 9095 | 19.84 | 17.82 |
| | | | | | 260 | 9192 | 25.81 | 12.75 | 523 | 9594 | 11.15 | 20.44 |
| | | | | | 270 | 9546 | 24.85 | 12.94 | 563 | 10093 | 13.25 | 20.38 |
| | | | | | 280 | 9899 | 19.74 | 14.66 | | | | |
| BA/ACR | 70 | 13502 | 12.05 | 17.45 | 350 | 12714 | 25.47 | 14.58 | 803 | 13112 | 17.98 | 18.95 |
| | 80 | 14131 | 9.97 | 18.32 | 360 | 13177 | 9.90 | 20.27 | 843 | 13504 | 36.47 | 12.17 |
| | 90 | 14377 | 15.02 | 16.03 | 370 | 13641 | 43.91 | 11.39 | 883 | 13867 | 49.34 | 9.74 |
| | 100 | 14622 | 14.13 | 13.71 | 380 | 14143 | 35.62 | 12.04 | 923 | 14230 | 48.87 | 10.03 |
| | 110 | 14868 | 23.89 | 13.71 | 390 | 14465 | 53.07 | 10.10 | 963 | 14569 | 63.32 | 8.12 |
| Heinrich Stadial 1 | 130 | 15359 | 21.54 | 15.48 | 400 | 15147 | 51.85 | 9.13 | 1043 | 15080 | 34.55 | 13.28 |
| | 150 | 15850 | 29.55 | 13.86 | 410 | 15469 | 56.22 | 8.74 | 1163 | 15643 | 43.56 | 11.53 |
| | 170 | 16341 | 26.16 | 20.62 | 420 | 16151 | 46.66 | 12.53 | 1243 | 16330 | 57.41 | 9.05 |
| | 190 | 16832 | 37.23 | 12.23 | 430 | 16653 | 52.94 | 11.59 | 1323 | 17065 | 59.96 | 9.09 |
| | 210 | 17215 | 30.68 | 17.35 | 440 | 17155 | 58.08 | 10.46 | | | | |
| | 230 | 17598 | 40.20 | 13.79 | 450 | 17657 | 55.73 | 9.79 | | | | |
| Last Glacial Max | 330 | 20095 | 39.40 | 15.56 | 500 | 20168 | 58.74 | 8.46 | NO RECORD | | | |
| | 340 | 20359 | 40.96 | 16.68 | 510 | 20670 | 60.88 | 8.21 | | | | |
| | 350 | 20623 | 39.68 | 13.74 | 520 | 21172 | 55.1 | 9.36 | | | | |
| | 370 | 20900 | 42.93 | 13.63 | 530 | 21674 | 58.49 | 10.06 | | | | |
| | 390 | 21178 | 35.89 | 14.61 | 540 | 22176 | 52.2 | 10.72 | | | | |
| | 410 | 21455 | 43.12 | 11.97 | | | | | | | | |
| | 430 | 21733 | 40.05 | 9.70 | | | | | | | | |
| | 450 | 22010 | 35.44 | 13.16 | | | | | | | | |

